Magnetic excitation spectrum of mixed-valence SmB_6 studied by neutron scattering on a single crystal

1995 J. Phys.: Condens. Matter 7 289

(http://iopscience.iop.org/0953-8984/7/2/007)

J. Phys.: Condens. Matter 7 (1995) 289–305. Printed in the UK

Magnetic excitation spectrum of mixed-valence SmB_6 studied by neutron scattering on a single crystal

P A Alekseev†, J-M Mignot‡, J Rossat-Mignod‡||, V N Lazukov†, I P Sadikov†, E S Konovalova§ and Yu B Paderno§

† Russian Research Centre (Kurchatov Institute), 123182 Moscow, Russia

‡ Laboratoire Léon Brillouin, CEA–CNRS, Centre d'Etudes de Saclay, 91191 Gif sur Yvette, France

§ Institute for Problems in Material Science, Ukrainian Academy of Science, 252180 Kiev, Ukraine

Received 27 June 1994

Abstract. The paramagnetic response of mixed-valence samarium hexaboride has been studied by inelastic neutron scattering using a low-absorption double-isotope single crystal of $^{154}Sm^{11}B_6$. Measurements were performed for energy transfers $0 \leqslant \hbar\omega \leqslant 50$ meV at temperatures ranging from 2 to 100 K. Two main contributions were observed in the spectra: a broad intermultiplet transition of single-ion type at $\hbar\omega \simeq 36$ meV, and a narrow low-energy excitation centred at $\hbar\omega \simeq 14$ meV, which is strongly anisotropic and temperature dependent and exhibits a weak but visible dispersion. The latter excitation appears to be an inherent feature of the mixed-valence state due to f-electron hybridization effects, which denotes the formation of a local bound state around the Sm sites.

1. Introduction

SmB_6 is a classical mixed-valence (MV) system which has been extensively studied since its discovery in the mid-1960s [1]. The main problem is the origin of the MV ground state of the Sm ion, which seems intimately connected with the formation of a narrow gap in the electronic density of states at the Fermi energy. The energy of the gap, determined by different methods, varied considerably: 2.7 meV by tunnelling spectroscopy [2], 5 meV from the temperature dependence of the electrical resistivity [3] and 16 meV by point-contact spectroscopy [4]. The average valence of Sm was established to be 2.56 [1, 5] at room temperature, and to vary slightly with T [6]. Several models have been proposed to interpret the intriguing properties of SmB_6. Mott [7] and later Martin and Allen [8] argued that, in the crystal structure of SmB_6, *on-site* f–d hybridization was indeed possible and could lead to the formation of a narrow gap and to an insulating ground state. On the other hand, Kasuya and his group [9] introduced the concept of 'Wigner crystallization in a Kondo lattice'. The main idea is that, because the concentration of carriers is low, the long-range Coulomb interaction between p electrons and holes can become equally important to or more important than their kinetic energy, allowing a local bound state to be formed [10]. Recently, Kikoin and Mishchenko [11] have proposed that an electronic instability can take place in semiconducting SmB_6, causing a transition to a quantum-mechanical MV state in Sm-based systems. This state is characterized by the appearance, in the homogeneous MV

|| Died during the completion of this work.

0953-8984/95/020289+17$19.50

phase, of a soft electronic exciton of intermediate radius, with mixed |4f)|5d) wavefunctions for the ground and excited states, which extends spatially to the nearest Sm ions.

The effects of charge and spin fluctuations on the lattice and magnetic dynamics of MV systems can be studied most thoroughly by inelastic neutron scattering, especially wherever since-crystal samples are available. In the case of SmB_6, however, a serious problem comes from the extremely large absorption of thermal neutrons by samples containing natural samarium and boron, making it necessary to use isotopically purified elements for the preparation of the crystals. Detailed measurements of the phonon excitation spectrum have been performed only recently [12], revealing a general softening of the modes (in comparison with the reference compound LaB_6) as well as clear anomalies in the acoustic branches, both of which could be interpreted in the framework of the exciton model of [11].

The search for specific features in the magnetic excitation spectrum due to the valence fluctuations was another challenging task. The first results for polycrystalline SmB_6 were published some years ago by Holland-Moritz and Kasaya [13]. These workers reported two peaks of magnetic origin to occur at $\hbar\omega = 15$ and 21 meV in spectra measured at liquid-helium temperature. Later, experiments performed on polycrystalline samples of SmB_6 and LaB_6 [14] confirmed the existence, for small momentum transfers, of an excitation centred at about 14 meV. Finally, three peaks were observed in the magnetic response function of SmB_6 in experiments performed on the time-of-flight spectrometer HET at the spallation neutron source ISIS [15]. One of them was quite narrow and visible only at low temperatures ($T < 100$ K); it was identified as the low-energy excitation reported previously, and its form factor was confirmed to decrease sharply with increasing momentum transfer. The other contributions, centred at $\hbar\omega \simeq 40$ meV and 130 meV, were reminiscent of the single-ion-type spin–orbit ('intermultiplet') excitations of the Sm^{2+} and Sm^{3+} configurations, respectively, but with considerable broadening ($\Gamma_{FWHM} \simeq 40$ meV, much larger than the instrumental resolution).

This paper describes the first experimental study of the magnetic dynamical response function of $^{154}Sm^{11}B_6$ measured by inelastic neutron scattering on a single crystal. Particular emphasis has been put on the wavevector and temperature dependences of the low-energy excitation, because this feature seems to be a characteristic of the MV ground-state wavefunction formed as a result of the hybridization of the local f state with the conduction band states. Some parts of this work have been briefly presented in conference reports [16, 17].

2. Experimental details

The single crystal of SmB_6 used in this study was the same sample used for previous investigations of the lattice dynamics [12]. The isotopic enrichment was 98.6% for Sm and 99.4% for B. The sample consisted of two coaligned plates (50 mm × 5 mm × 2 mm), with a resulting mosaicity $\Gamma_{FWHM} \simeq 20$–$25'$, as deduced from rocking curves performed on the nuclear Bragg peaks. The room-temperature lattice parameter obtained by x-ray diffraction was $a = 4.133\,9(2)$ Å. Measurements of the magnetic excitation spectra were carried out on the high-luminosity three-axis spectrometer 2T at the Laboratoire Léon Brillouin [16]. Energy scans at fixed scattering vector Q were performed in the so-called 'constant-k_f' mode, for which the neutron counts in the detector are essentially proportional to the scattering function (neglecting higher-order beam contaminations). In order to achieve either higher-energy transfers or better resolutions, two different neutron energies $E_f = 30.4$ meV ($k_f = 3.834$ Å^{-1}) or $E_f = 14.7$ meV ($k_f = 2.662$ Å^{-1}) were selected from the graphite-filtered scattered beam by means of a PG(002) analyser, in combination with a Cu(111) or

PG(002) double-curvature monochromator, respectively. The resulting energy resolutions, estimated from the linewidth Γ_{FWHM} of the incoherent elastic peak, were 2.0 meV for $k_f = 3.834$ Å^{-1} and 1.0 meV for $k_f = 2.662$ Å^{-1}. The sample was oriented with all three principal symmetry directions within the scattering plane, and cooled to the desired temperature (2–100 K) using an ILL-type 'orange' cryostat. Owing to the slab geometry of the sample and to its relatively strong residual absorption, special attention was paid to the dependence of the sample transmission on its orientation with respect to the incoming and outgoing neutron beam directions. From a preliminary elastic scan in which the sample was rotated by 95°, it was ascertained that, for angles between $k_i(k_f)$ and the sample plane larger than 10°, the variation in the intensity remained within the limits of 15%. These angles were controlled during the measurements, and none of them was allowed to become smaller than typically 20°. The experimental inelastic spectra have been fitted to a paramagnetic scattering law of the form

$$S(\hbar\omega, T) \propto \hbar\omega/[1 - \exp(-\hbar\omega/k_B T]P(\hbar\omega, T)$$

where $P(\hbar\omega, T)$ is a linear combination of Lorentzian or Gaussian spectral functions.

3. Results

Two excitations have been studied in these experiments: firstly the lowest intermultiplet transition, $[J = 0] \rightarrow [J = 1]$, of Sm^{2+}, occurring at an energy of about 36 meV; secondly the new excitation at 14 meV, which is observed at low temperatures and for small momentum transfers ($Q \equiv |Q| < 2$ Å^{-1}). Both contributions have been shown, from inelastic neutron scattering measurements on a polycrystalline sample, to be characteristic features of the magnetic excitation spectrum of samarium [14, 15].

3.1. Intermultiplet transition

One of the goals of the present experiments was to establish the linewidth of the 36 meV excitation, whose energy [15, 16] corresponds to the transition $^7F_0 \rightarrow {}^7F_1$ of the Sm^{2+} configuration. By using a single crystal, one can distinguish this intrinsic broadening from the effects connected with a possible energy dispersion of the excitation. Our measurements have been performed for different values of the scattering vector Q, in particular at a Γ point and at the zone boundary [16], No evidence for dispersion was found but considerable damping ($\Gamma/2$ was very much greater than the instrumental resolution) was confirmed to occur for temperatures as low as 2 K. Spectra obtained for two different scattering vectors $Q = (q, q, q)$ along the [111] direction are displayed in figure 1.

The curve corresponding to $q = 1.25$ (figure 1(a)) is actually a combination of data points obtained for slightly different values of q in longitudinal geometry. This procedure allows us to separate the magnetic contribution from that due to optical phonons, by taking advantage of their steep energy dispersion [12]. Appropriate scaling has been applied, using the curve shown in the inset, to account for the minor ($\simeq \pm 10\%$) variation in the form factor with Q (3.1 Å$^{-1} \leqslant Q \leqslant 3.4$ Å^{-1}). Two peaks are observed in this spectrum: a narrow peak at about 10 meV corresponding to a longitudinal acoustic phonon mode [12], and a broad peak at around 36 meV, corresponding to the intermultiplet transition. It is obvious that the background correction plays an important role in determining the linewidth. Our experimental estimate, made at large Q-values, is based on the observation that this background is almost independent of the sample orientation and energy transfer in the range

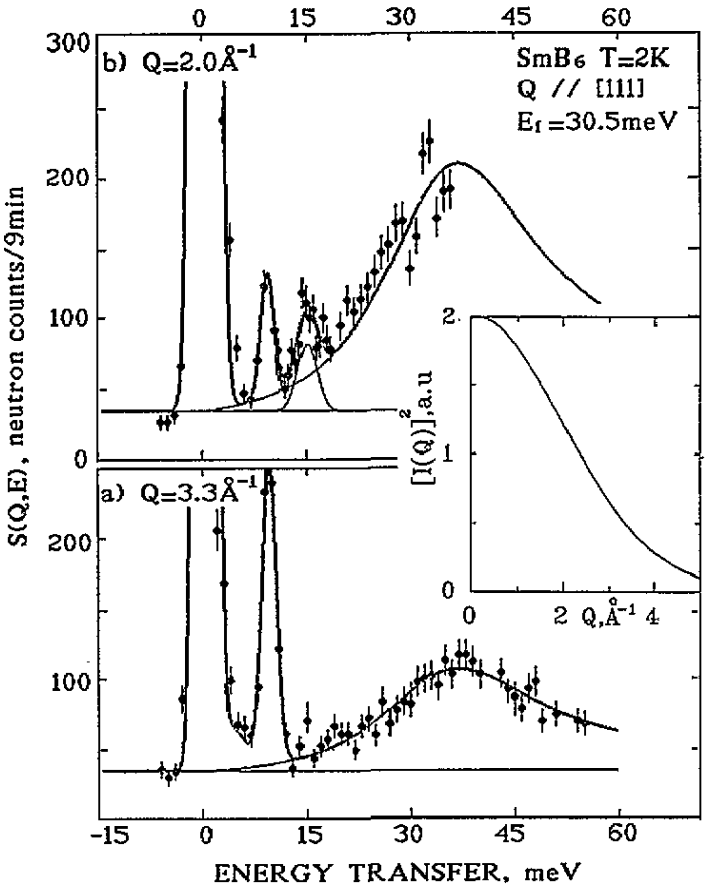

Figure 1. Neutron scattering spectra of single-crystal SmB_6 at $T = 2$ K measured at constant k_f ($E_f = 30.5$ meV), for scattering vectors $Q = (q, q, q)$. (*a*) $q = 1.25$ ($Q = 3.3$ Å^{-1}); most of the experimental data points between 32 and 51 meV are from measurements done at $q = 1.17$ and at 1.30, scaled according to the form factor of the $J = 0 \rightarrow J = 1$ intermultiplet transition (see text). The peak at $\hbar\omega = 10$ meV is due to a LA-phonon mode. The solid line is the best fit by a single Lorentzian in the energy range 16–55 meV: $\Gamma/2 = 14$ meV; $E_0 = 34.5$ meV. (*b*) $q = 0.76$ ($Q = 2.0$ Å^{-1}); the limited energy range is due to restrictions in the scattering geometry. The two low-energy peaks (LA phonon at about 10 meV and magnetic excitation at about 15 meV are fitted by Gaussians. The solid line through the high-energy peak corresponds to the Lorentzian spectral function obtained in (*a*), scaled by a factor 2.35 in intensity according to the form factor of the intermultiplet transition. The thin lines in (*a*) and (*b*) represent the background. The inset shows the calculated dipole inelastic structure factor (proportional to the form factor) of the $^7F_0 \rightarrow {}^7F_1$ intermultiplet (spin–orbit) transitions. (After [31].)

of instrumental configurations used for the present measurements. Its value is shown by thin lines in figure 1. The broad peak was fitted assuming a single Lorentzian shape for the spectral function, yielding a half-width $\Gamma/2 \simeq 14$ meV.

The results obtained for a smaller momentum transfer, $q = 0.76$, along the same direction are shown in figure 1(*b*). This spectrum and the previous spectrum correspond to equivalent positions in the Brillouin zone, half-way to the zone boundary, but Q is now equal to 2.2 Å^{-1}, and the energy transfer is limited accordingly to $\hbar\omega \leqslant 40$ meV.

In figure 1(*b*), the broad peak drawn as a continuous line is *not* a fit to the data but was obtained by scaling the curve in figure 1(*a*) according to the calculated form factor of the intermultiplet transition. The agreement observed further supports the procedure used above to combine different spectra. Let us emphasize again that no evidence for dispersion was found in the present results, nor by comparing them with spectra corresponding to different points in the Brillouin zone obtained in previous measurements [16].

By comparing the low-energy part of the spectra in figure 1, one notes that, in addition to the phonon contribution, whose intensity varies as Q^2, another narrow peak appears at an energy of about 15 meV in the data for $Q = 2.2$ Å^{-1}, whereas it does not exist for $Q = 3.3$ Å^{-1}, although the measurements correspond to equivalent points in the Brillouin zone. This intriguing feature, already reported previously [14–16], is the subject of the following section.

3.2. *Low-energy excitation*

A key to understanding the origin of this contribution to the spectral function is provided by a careful examination of its dependence on the absolute value and orientation of the scattering vector, as well as of temperature effects.

3.2.1. Scattering-vector dependence. Since it had been established earlier that the intensity of this excitation is largest at low temperatures, its Q-dependence was studied most thoroughly at $T = 2$ K. By comparing intensities obtained at equivalent reciprocal-space points for different Q-values, it can be concluded that the variations in the intensity depend on the momentum transfer Q rather than on the reduced wavevector q and thus correspond primarily to changes in the form factor of the excitation. This is clearly demonstrated by the plots in figure 2 since firstly the spectra measured for $Q = q + G_{(011)}$ (curve a) and $Q = q + G_{(111)}$ (curve b), corresponding to the *same* reduced wavevector $q = (0, -0.3, -0.3)$, display quite different intensities for the peak at 14 meV, and secondly the latter difference cannot be ascribed to the difference in the angles between the scattering vector and q (polarization) because the effect is reversed (i.e. lower intensity for longitudinal geometry, $Q \| q$) between for $Q = (-0.25, -0.25, -0.25) + G_{(111)}$ (longitudinal, curve c) and $Q = (-0.25, 0.25, 0.25) + G_{(100)}$ (transverse, curve d).

Figure 3 shows selected experimental runs for Q parallel to [111]. The shaded areas represent a fit of the excitation by a Gaussian lineshape (width corresponding to the instrumental resolution). A strong variation in the intensity is observed as a function of Q, with only a minor change in the excitation energy. The Q-dependences of the integrated intensity for all directions measured are collected in figure 4. The corresponding map of the $(0\bar{1}1)$ plane is shown in the inset. Clearly, the intensity is largest for $Q \|$ [111], is much weaker along [011] and almost disppaears when in the direction [100]. It also exhibits a surprisingly fast decrease with increasing Q and almost vanishes for $Q > 2$ Å^{-1}. Furthermore, the present results indicate that a *maximum* exists at small Q. This maximum is most pronounced for $Q \|$ [111], where its position coincides with the zone boundary. This coincidence does not hold true for other directions of Q. It is interesting to compare the Q-dependence of the intensity with that of the excitation energy $\hbar\omega$. The results for two particular directions [111] and [011] of the scattering vector are shown in figure 5. In both cases, $\hbar\omega$ varies rather weakly but displays a definite minimum at the *same* energy where the intensity is largest.

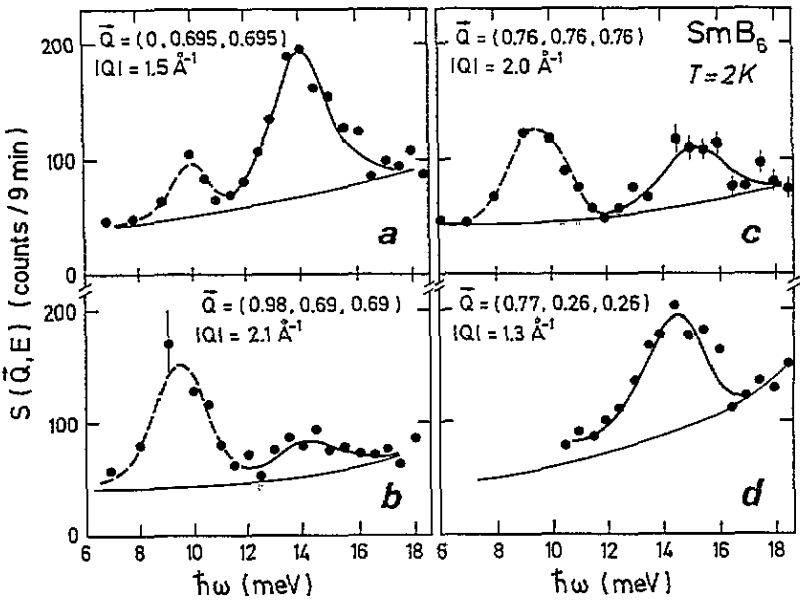

Figure 2. Comparison of energy spectra at $T = 2$ K for couples of scattering vectors corresponding to equivalent q-values: (*a*) $q \simeq (0, -0.3, -0.3)$; (*b*) $q \simeq (-0.25, \pm 0.25, \pm 0.25)$. The experimental conditions are the same as in figure 1. The lines are guides to the eye.

3.2.2. Temperature dependence. As already noted, the width of the excitation at 14 meV at liquid-helium temperature is of the order of the experimental resolution, a striking result in comparison with the strong broadening exhibited (at all temperatures) by the intermultiplet transitions. In the present case, both the intensity and the width of the excitation change drastically when temperature rises. The effect of varying temperature was studied for a number of different Q-values, especially those corresponding to the largest intensity. Figure 6 shows the results obtained for $Q = (0.5, 0.5, 0.5)$ ($Q = 1.3$ Å^{-1}). The background was derived from measurements for different scattering vectors; in addition to the true (essentially energy-independent) instrumental contribution, one notes an inclined baseline which originates mainly from the low-energy tail of the intermultiplet transition peak. Model calculations using a Lorentzian spectral function (see section 1) for the intermultiplet transition show that, when the temperature is raised from 0 to 100 K, the magnetic scattering intensity increases by less than 30% with respect to $T = 0$ K in the energy range of interest, 6–20 meV. This corresponds to an increase in the total intensity (magnetic+background) at $T \simeq 100$ K by at most 10% at 6 meV and 5% at 20 meV. The contribution from the flat part of the LA phonon branch has been modelled by a Gaussian centred at $\hbar\omega \simeq 10$ meV, whose intensity is scaled by the Bose population factor. The temperature dependence of the fit parameters obtained for the magnetic peak is shown in figure 7. The FWHM corresponds to the experimental width of the magnetic peak. It was derived from a Gaussian fit at the lowest temperatures, where the shape of the line is determined by the resolution function of the spectrometer, and from a Lorentzian fit at higher temperatures where the intrinsic linewidth is obviously dominant. The temperature behaviour displayed in figure 7 for $Q = (0.5, 0.5, 0.5)$ is representative of that measured for other scattering vectors.

An interesting point is that an additional featureless contribution, superimposed on the background, appears at temperatures $T \geqslant 50$ K especially in the energy range $\hbar\omega \simeq 5$–

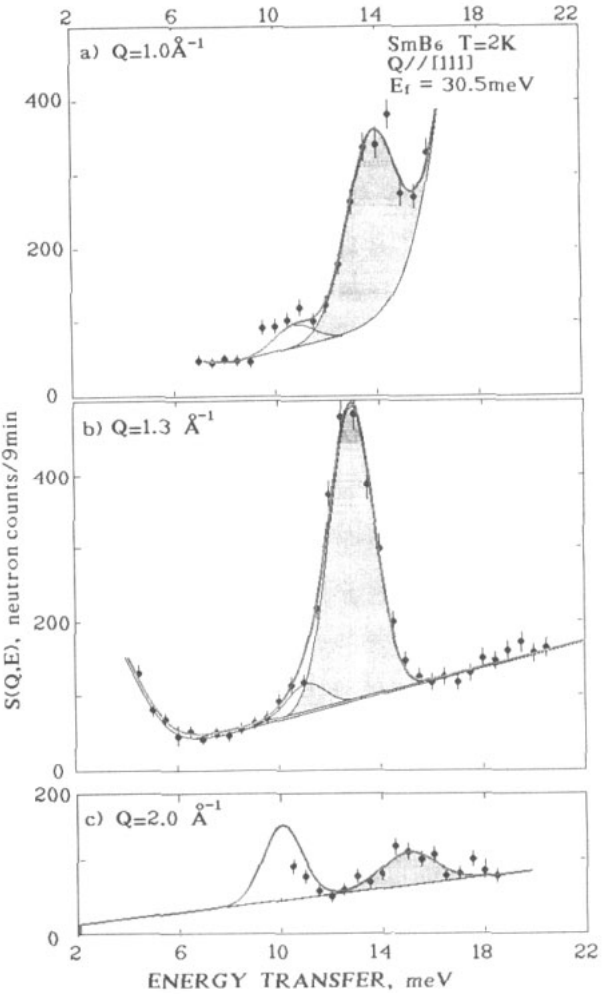

Figure 3. Q-dependence of the 14 meV inelastic peak at $T = 2$ K for scattering vectors $\boldsymbol{Q} = (q, q, q)$ where (*a*) $q = 0.38$, (*b*) $q = 0.49$ and (*c*) $q = 0.76$, measured at constant k_f ($E_f = 30.5$ meV). The shaded areas represent fits by Gaussians.

8 meV (figure 6). At 100 K, its intensity becomes approximately equal to the initial background value. A quantitative estimate of the possible contamination from incoherent phonon scattering rules out this channel as a possible source of the intensity observed (recalling that the ratio σ_c/σ_i of the nuclear cross sections is about 35 for SmB_6), and the additional contribution is thus most probably magnetic in origin. In the fits for temperatures $T \geqslant 50$ K displayed in figure 8, this extra term was approximated by a quasi-elastic Lorentzian. In order to separate it from the foot of the elastic peak for energy transfers smaller than 10 meV, measurements with higher energy resolution ($E_f = 14.7$ meV) were performed at $T = 2$ and 103 K along two main symmetry directions [100] and [111]. Several spectra corresponding to values of Q between 1.0 and 3.3 Å^{-1} were measured for $\boldsymbol{Q}$ parallel to the [111] direction, where the experimental conditions are more favourable. The main experimental observations can be summarized as follows. The intensity of the

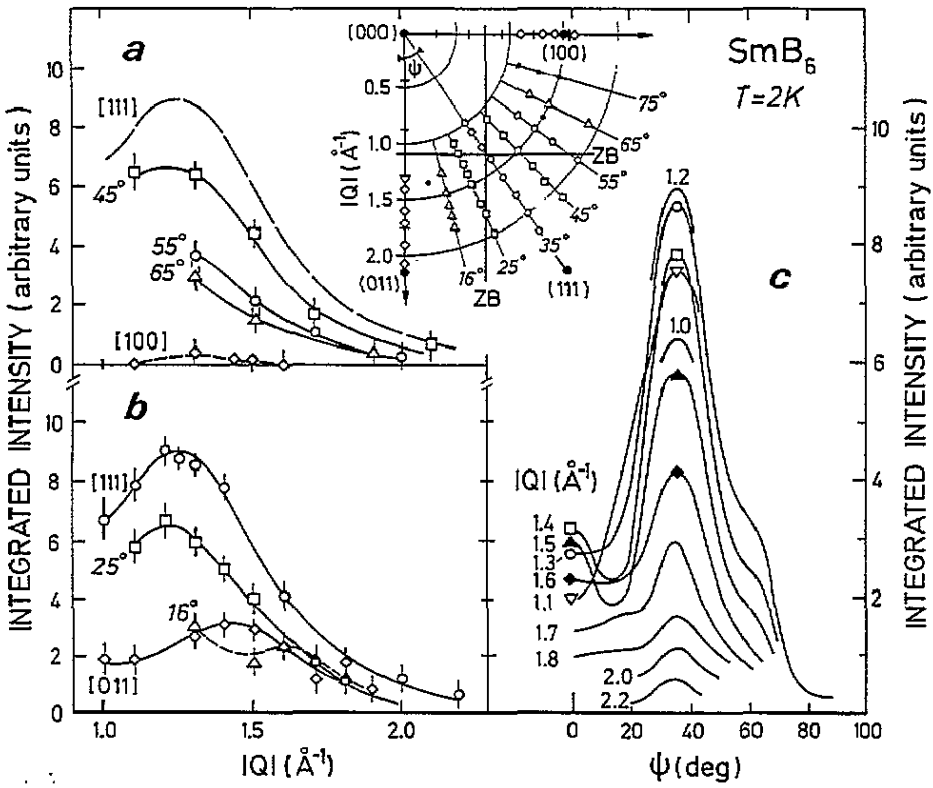

Figure 4. Integrated intensity of the low-energy excitation plotted (*a*),(*b*) as a function of Q for selected directions of the scattering vector withi the $(0\bar{1}1)$ plane and (*c*) as a function of the angle with respect to the [011] direction for selected Q-values. The scattering plane is represented in the inset, with symbols denoting the Q-values at which measurements have been made.

aforementioned high-temperature contribution does not vary appreciably with increasing Q up to highest measured value of 3.3 Å^{-1}, in contrast with the steep decrease reported above for the 14 meV excitation at $T = 2$ K, nor is there evidence for any sizable anisotropy. No reproducible structure was observed for this scattering intensity in the energy range 2–15 meV. The spectrum at $T = 103$ K, corrected from the background and the phonon contribution, is shown in figure 8 for one particular scattering vector $Q = (0.527, 0.527, 0.527)$. Longer counting times were used to compensate the loss of intensity resulting from the change in experimental conditions. The background was obtained from the low-temperature run, after subtracting out the 14 meV magnetic peak. Within error bars, the spectrum can be approximated by a quasi-elastic Lorentzian with a width of $\Gamma/2 = 11$ meV, as shown by the solid line in figure 8.

4. Discussion

The Q-dependence of the intensity of the intermultiplet transition follows quite well the calculated inelastic structure factor. No significant dispersion could be detected. Let us recall that, in a previous time-of-flight experiment [15], both the excitation discussed here, corresponding to the $4f^6$ configuration of Sm^{2+} ($^7F_0 \rightarrow {}^7F_1$), and a second excitation, at

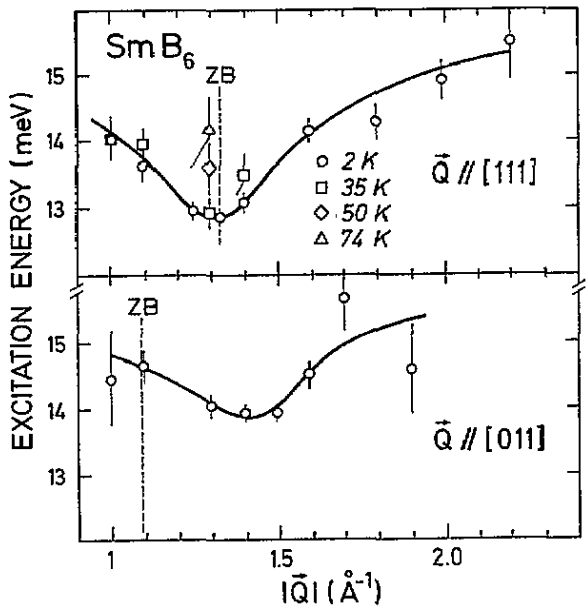

Figure 5. Variation in $\hbar\omega$ for the low-energy excitation as a function of Q: (*a*) $Q\|$ [111]; (*b*) $Q\|$ [011]. The solid lines are guides to the eye.

about 130 meV, corresponding to the $4f^5$ configuration of Sm^{3+} ($^6H_{5/2} \rightarrow {}^6H_{7/2}$), had been observed, with an intensity ratio in accordance with the valence state of Sm derived from x-ray absorption spectroscopy. All these results can thus be understood, in an atomic-like picture, by assuming a simple superposition of the contributions from the two adjacent valence states of Sm. On the other hand, the intrinsic linewidth $\Gamma_{FWHM} = 28$ meV of the lower intermultiplet transition derived from the present measurements is much larger than the instrumental resolution at this energy transfer (about 4 meV). This broadening cannot result from a splitting of the $J = 1$ excited state of Sm^{2+} by the crystal electric field (CEF), since the local cubic symmetry of the rare-earth site does not allow any splitting of the triplet. We rather believe that the linewidth is related to the short lifetime of the single-ion state of Sm, which can be estimated as $\tau_f = 2\hbar/\Gamma = 3 \times 10^{-13}$ s at $T = 2$ K. In [15], the widths of the two intermultiplet transitions were estimated to be close to each other, suggesting that the origin of the broadening is the same for both configurations of the Sm 4f shell. This time–energy scale can be regarded as an estimate of the rate of interconfiguration fluctuations, or as a measure of the uncertainty in defining the MV system under investigation in terms of the parent wavefunctions of the ionic states.

Concerning the low-energy excitation, the bulk of experimental evidence indicates that it cannot originate from either of the Sm ionic configurations. At first glance, one might be tempted to invoke some CEF excitation within the $J = \frac{5}{2}$ multiplet. However, in addition to the strong damping expected from the preceding discussion, this would be in contradiction to the observed Q-dependence of the intensity. The drop at large Q is much too fast to be consistent with a localized f-electron form factor (for Sm^{3+}, it should extend up to 4 $Å^{-1}$). Furthermore, the temperature variation expected for a doublet–quartet transition (whichever of these states is the lowest) is much slower than observed experimentally. The latter discrepancy is illustrated in figure 7 for the case of a Γ_7 ground-state doublet. Moreover, the experimental anisotropy cannot be accounted for in a simple CEF model. It is

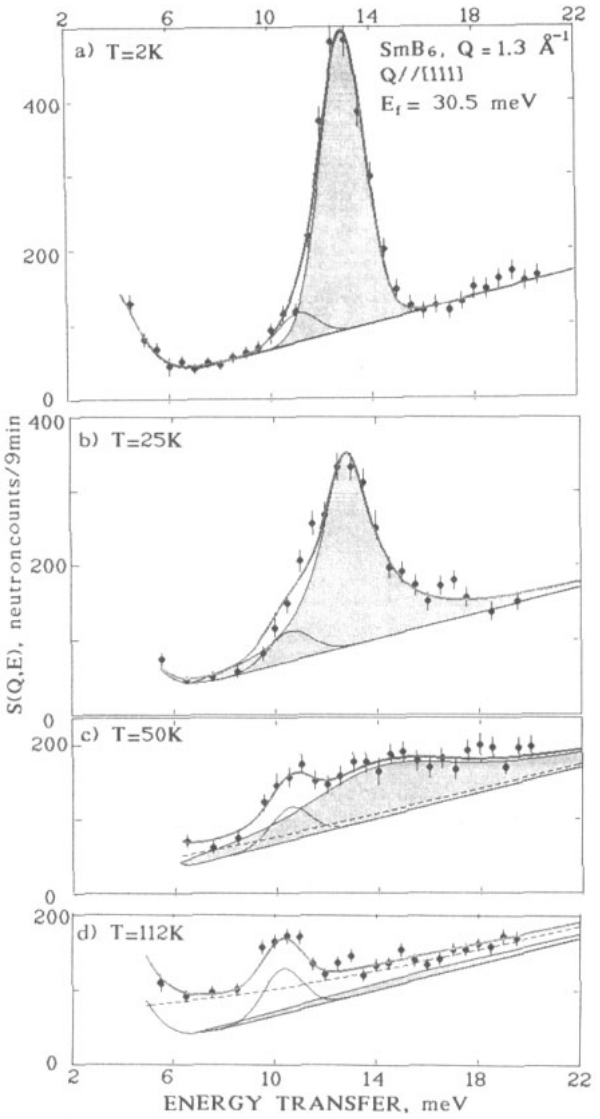

Figure 6. Temperature dependence of the low-energy excitation measured at constant k_f (E_f = 30.5 meV) for Q = 1.3 Å^{-1} along the [111] direction. The shaded areas represent fits by Lorentzian of Gaussian lineshapes depending on temperature (see text). The phonon contribution at $\hbar\omega \simeq 10$ meV was scaled between T = 2 and 112 K according to the Bose temperature factor. The background was determined from the data at T = 2 K and assumed to be temperature independent. The dashed lines for T = 30 and 112 K represent the additional quasi-elastic contribution discussed in the text.

even difficult to explain the results by assuming some interplay between CEF excitations and another type of excitation, e.g. phonons, because the 14 meV peak lies just within the energy gap between the acoustic branches and the lowest optical branches, and because its energy dispersion and change in intensity as a function of the reduced wavevector q are weak. Furthermore LA and TA phonons do not show any evidence, in their Q- or T-dependences,

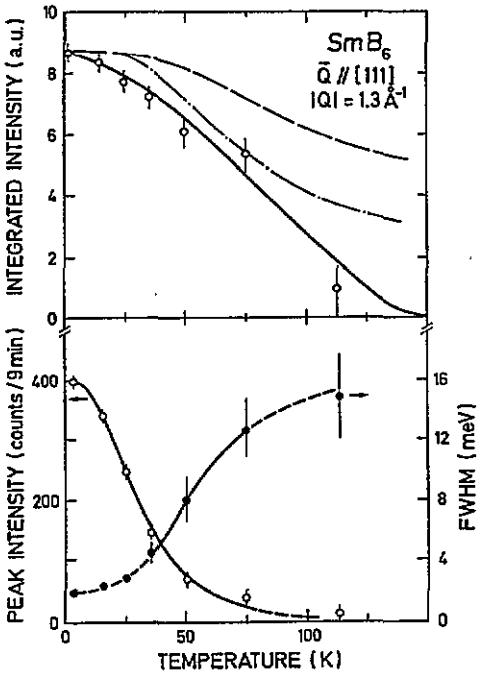

Figure 7. Temperature dependences of parameters of the low-energy excitation deduced from the fits in figure 5: (*a*) integrated intensity (dashed and dashed-dotted lines correspond to model calculations for energy level schemes consisting of two crystal-field states Γ_7–Γ_8, or a singlet and a sextuplet, respectively; see text); (*b*) peak intensity (open circles) and linewidth Γ_{FWHM} (full circles). The lines are guides to the eye.

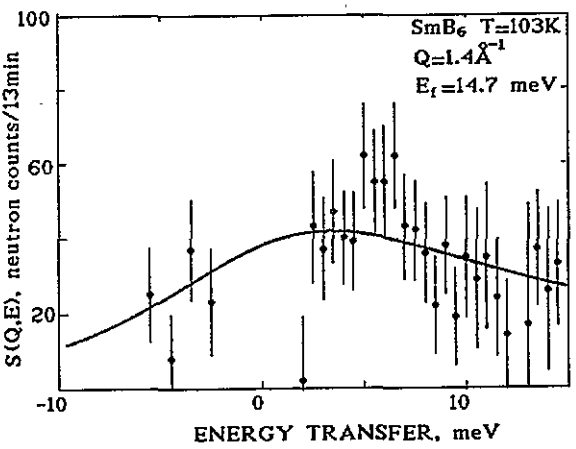

Figure 8. Difference spectrum between the data at 103 and 2 K for $Q = 1.4$ Å^{-1} along the [111] direction. The magnetic and phonon peaks in both spectra were subtracted out beforehand. The solid line corresponds to a scattering function consisting of a single quasi-elastic Lorentzian ($\Gamma/2 = 12$ meV).

of an admixture with magnetic modes [18]. We are thus led to the conclusion that the new excitation is a genuine feature of the MV state of Sm. Its remarkable narrowness at low temperatures suggests that it corresponds to a true eigenstate of the system, in contrast with the integral-valence configurations whose intermultiplet transitions appear considerably damped.

From our detailed experimental study of the 14 meV transition, we can now infer some of the characteristics of this new state. The very restricted range of momentum transfer ($Q \leqslant 2$ Å^{-1}) in which it is observable indicates that the electron density extends radially much farther than expected for atomic 4f electrons. The anisotropy of the intensity distribution (i.e. strongest along the [111] direction for all Q-values) shows that it is concentrated near the directions pointing towards the centres of the neighbouring boron octahedra. Along these directions, the electron density can be estimated to be maximum at a distance of about 1.5–2 Å from the Sm site, three times larger than the radius of the 4f shell. This behaviour appears to reflect the mixing of the 4f wavefunctions of the rare earth with the d or p states of its neighbours, leading to a loosely bound state around the Sm site. From figure 4(c), the distribution of the magnetic scattering intensity in Q-space can be described, as a first approximation, as symmetric with respect to the [111] direction. However, some deviation is observed near the direction joining the Sm atom to its nearest boron neighbour (about 16° from [011]; see figures 4(a) and 4(b)). This result suggests that the boron wavefunctions contribute to the formation of the extended electronic state.

The maximum observed, for several directions of Q, in the variation in the intensity (figures 4(a) and 4(b)), and its correlation with the weak but definite dispersion of the peak energy, especially for $Q \parallel$ [111] and [011] (comparison of figures 4(a) and 4(b) with figure 5), can be ascribed to the spatially coherent motion of the exciton state, whose extension is probably limited to the first samarium neighbours.

Since no evidence was found for a change in the anisotropy of the 14 meV peak as a function of temperature we shall focus on the T-variation in its intensity and linewidth measured for one particular scattering vector, $Q = (0.5, 0.5, 0.5)$ as displayed in figure 7. An observable increase in the linewidth can already be detected at temperatures as low as 20 K (the resolution of about 2 meV masks a possible variation at lower temperatures) and is followed by a decrease in the integrated intensity, both of which result in a dramatic drop of the peak intensity, by about an order of magnitude, at $T \simeq 50$ K. Most probably the more isotropic quasi-elastic contribution starts to form in this temperature range.

Concerning the energy dispersion mentioned above for $Q \parallel$ [111], no appreciable change occurs up to $T = 35$ K (figure 5). At higher temperatures, the excitation energy $\hbar\omega$ for $Q = (0.5, 0.5, 0.5)$ (position of the minimum at $T = 2$ K) increases, as can be seen for $T = 50$ K and 70 K, causing the dip in the dispersion curve to disappear.

To understand the quasi-elastic scattering observed in the spectra at about 100 K, let us first compare it with what would be expected from the integral valence states of samarium. In the case of Sm^{2+}, the possible contribution to the quasi-elastic scattering arising from the thermal population of the $J = 1$ excited spin–orbit state at 100 K is small; its intensity may be estimated to be about 1.5% of that of the $^7F_0 \rightarrow {}^7F_1$ intermultiplet transition, approximately 5 counts in figure 8, assuming a similar linewidth. On the other hand, the Q-dependence of the quasi-elastic intensity, showing no strong decrease up to $Q \simeq 3.3$ Å^{-1}, is compatible with a $Sm^{3+}\,{}^6H_{5/2}$ form factor, which rises weakly up to about 4 Å^{-1} and begins to fall only at larger momentum transfers. The estimated cross section in this channel for the actual valence mixing (54% of Sm^{3+}) is of the order of 0.2 b, which is consistent with the experimental data. However, this picture completely fails to explain the drop in the quasi-elastic magnetic scattering which occurs when the system is cooled to liquid-helium

temperature. We note that, although its intensity is relatively small, such a contribution would be clearly seen in the spectra at $T = 2$ K, so long as its linewidth remained typically of the order of a few millielectronvolts.

The occurrence of a singlet ground state, already derived from other types of measurement, is thus a key point in understanding the temperature dependence of the magnetic excitations in SmB_6. Let us emphasize, however, that the 14 meV excitation cannot be ascribed to a simple one-electron transition from a singlet ground state within the Sm^{3+} ionic state since, assuming an excited state with sixfold degeneracy, the drop in the intensity with increasing temperature expected from thermal population effects (dashed–dotted line in figure 7(*a*)) would differ substantially from what is observed experimentally. This further supports our conclusion that the new excitation cannot arise from simple atomic-like electron states with an energy splitting of 14 meV, but rather involves an interaction between the 4f electrons of Sm and another electron subsystem.

One possible mechanism is the hybridization of the 4f states with the conduction band whose properties vary strongly in this temperature range owing to the existence of a narrow gap in the electronic density of states [19]. From ^{11}B NMR experiments [20], two distinct regimes, differing in their temperature dependences of the relaxation rate, could be defined as a function of temperature, with a boundary at approximately 15 K. The small gap in the conduction band at the Fermi energy was suggested to be responsible for the behaviour at $T \geqslant 15$ K. However, if one supposes that the electronic hybridization gap is less than 14 meV, the conduction electron–f-electron exchange relaxation mechanism should not be sufficient to produce a broadening of the magnetic excitation at energy $\hbar\omega \simeq 14$ meV as is observed above 20 K. If, on the other hand, the gap is larger than 14 meV, then the relaxation will become effective only at temperature higher than 100 K. In both cases, no strong damping of the excitation is expected in the 14 meV range at low temperatures. We are thus led to the conclusion that the T-dependence observed experimentally results from a change in the properties of the MV eigenstate of SmB_6 occurring at temperatures of the order of 40 K. It may indicate that the excitonic-like local state is a specific feature of the low-carrier regime and becomes unstable when even a small number of carriers are thermally excited across the gap.

It is interesting to compare the present results with previous studies of the magnetic dynamical response in other Sm-based MV systems. A broad magnetic peak at an energy transfer of about 35 meV was obtained for $Sm_{0.75}Y_{0.25}S$ in time-of-flight experiments using a polycrystal [21]. Its large width was interpreted as due to the interaction between the intermultiplet transition and an optical phonon mode of the same symmetry, but not direct experimental evidence for a dispersion of the intermultiplet transition has been obtained from single-crystal measurements. The lowest Q-value in the experimental spectra presented in [21] was 2 $Å^{-1}$, so that an excitation of the type observed in SmB_6 at 14 meV could have been overlooked. Another series of experiments, using the same sample, was performed at the ILL on the time-of-flight spectrometer IN6. In that case, the neutron energy loss spectrum was limited to only a few millielectronvolts [22] restricting the analysis to the neutron energy gain side. These workers detected some quasi-elastic scattering in spectra measured at temperatures higher than 100 K, and the associated form factor at $T = 250$ K had Sm^{2+} character. The latter result could be explained by the admixture of the Sm^{2+} ($J = 1$) state, which has a large cross section, into the original Sm^{3+} ($J = \frac{5}{2}$) state at elevated temperatures. These workers also suggested, from their data analysis, that some intensity was removed from the quasi-elastic scattering at lower temperatures and should be transferred to another component of the spectrum. Therefore, in both experiments, the

conditions were not favourable for observing a low-energy excitation such as that in SmB_6 but its existence cannot be ruled out.

On the other hand, striking similarities exist, in the static properties, between the MV phases of SmS and SmB_6. It is well known (not but well understood) that the induced magnetic form factor of Sm in MV SmS is identical with that of Sm^{2+} [23]. Recently, we obtained the same result in polarized-neutron elastic scattering experiments on SmB_6 at low temperatures [24]. It is important to note that, in these measurements, the first magnetic reflection in $Q = (1, 0, 0)$ already corresponds to a momentum transfer of about 1.5 Å^{-1} (and to a direction of reciprocal space, $Q\|$ [100], in which the intensity of the 14 meV inelastic peak has been found to vanish). So the conditions are again quite unfavourable for observing a possible contribution in the elastic response from the extended electron state around Sm.

TmSe is another well known MV compound with a narrow gap in its electronic density of states, whose ground state has been shown to be antiferromagnetic. In the paramagnetic region, a narrow peak has been observed in the neutron scattering spectra at $\hbar\omega = 10$ meV [25]. The energy dispersion of this excitation is weak, but its intensity falls off rapidly in the Q-range 1.6–2.2 Å^{-1}, and also for temperatures higher than 30 K. Despite these analogies, TmSe probably needs to be treated as a distinct case, since its ground state is clearly degenerate, in contrast with the MV Sm systems discussed above.

Finally, it has been argued recently [26] that the 'localized homogeneous MV state' picture proposed for SmB_6 can be applied to the 'Kondo insulator' CeNiSn and accounts for the neutron scattering results reported for this system [27, 28].

In summary, the results of existing experiments for several MV systems reveal some similarities between their magnetic excitation spectra and those of SmB_6. It is thus tempting to assume that the specific properties of the ground-state wavefunction of SmB_6 which have been discussed above reflect some more general features of the MV state in low-carrier compounds.

Until recently, only a few theoretical studies [29, 30] had addressed the question of the magnetic excitation spectrum of semiconducting MV systems. On the assumption that a 'hybridization gap' Δ exists in such systems [8], these workers calculated the two-particle Green function for the Anderson lattice Hamiltonian with on-site hybridization and predicted an inelastic peak to occur at an energy $\hbar\omega \simeq \Delta$ in the magnetic dynamic response function at low temperatures. The origin of this behaviour is simply the excitation of the 4f electrons through the hybridization gap, whose intensity is expected to be maximum when q is close to the zone boundary (peaks in the single-particle density of states). Quasi-elastic scattering is also expected to appear when the temperature increases because excitations without crossing the gap become possible. However, these calculations require the 4f level to lie within the gap or at least close to it and assume an electron concentration of two carriers per site, which is not realistic for the systems under consideration. The existence of pronounced peak structures in the electronic density of states at the gap edges has also been questioned by more recent calculations.

With respect to the experiments, the above calculations predict a temperature variation in the excitation which is qualitatively similar to that found in SmB_6 and can also account for the weak Q-dependence of its energy $\hbar\omega$. Nevertheless, two main features, namely the small intrinsic linewidth and the anisotropy of form factor which reflects the non-local character of the MV wavefunction, cannot be explained simply in the framework of the pure on-site f–d hybridization assumed by these models.

The theories based on the idea of an excitonic semiconducting state represent an attractive alternative. In the 'homogeneous' model of [11], the MV ground-state

wavefunction consists of two components: one corresponds to a localized f orbital of the central site, and the other to a loosely bound state $B_m^{(f)}$ expressed as a linear combination, with appropriate symmetry, of d or p orbitals from the neighbouring Sm and/or B atoms. Spin excitations within the latter spatially extended component are considered responsible for the 14 meV peak and its strongly Q-dependent form factor. For a plausible form of B_m^f, the experimental anisotropy of the peak intensity can be qualitatively reproduced. The energy dispersion is ascribed to the coherent character of the magnetic excitation, owing to the overlap between the extended wavefunctions from neighbouring sites. The remarkable narrowness of the 14 meV peak, in contrast with the intermultiplet transitions, is interpreted as evidence that the former arises from a true eigenstate of the system, whereas the latter merely persist in the form of resonances, reminiscent of the magnetic response of the parent integral valence states.

In Kasuya's [10] model, a somewhat more complex electron transfer mechanism is invoked, based on the remark that the f hole produced by the conduction electron–f-electron mixing must be screened primarily by a d-electron, forming a so-called d-wave bonding Kondo state with fairly high binding energy (of the order of several electronvolts). The extended bound state observed by neutron scattering is then ascribed to an f-wave bonding Kondo state formed by the Coulomb interaction between the hole with d symmetry and the conduction electron with f symmetry created at the previous stage of the process. Central to this model is the idea that, in such 'low-carrier' systems, the Coulomb interaction can overcome the kinetic energy of conduction electrons. It should also be noted that this picture assumes an inhomogeneous mixture of Sm^{2+} and Sm^{3+} states (Wigner crystallization), although mechanisms for interchanging divalent and trivalent sites has also been proposed ('Wigner liquid').

From the experimental point of view, the latter two models agree on the existence of a local bound state as well as on ascribing the narrow 14 meV peak to a magnetic excitation from this ground state. The form factor dependence is regarded as evidence of the dominant contribution of the p (d) orbitals of the B (Sm) near neighbours to the extended wavefunction, and the dispersion is ascribed to coherence established at low temperatures among excitonic states at different sites. Major differences exist, however, not only in the detailed microscopic description of the MV wavefunction but also in the nature of the magnetic excitation observed by neutrons: moment reversal, spin–orbit excitation in [11] or transition from a singlet Kondo state to a magnetic (s-symmetry exciton) state in [10]. Although these theories have not yet come to a point where they can be compared quantitatively with experiments, in particular regarding the key point of the temperature dependences, it seems that they imply quite different behaviours as a function of the valence state of Sm, which could be tested experimentally. Neutron scattering measurements have been undertaken along this line on La-substituted systems, and their results will be discussed in a forthcoming paper.

5. Conclusion

The main conclusions of our experimental study can be summarized as follows. The magnetic response function of SmB_6, obtained by inelastic neutron scattering, includes two types of contribution: spin–orbit transitions corresponding to the spectra of the 'parent' integral-valence states $4f^5$ and $4f^6$; an inelastic peak at $\hbar\omega = 14$ meV, which we ascribe to magnetic excitations from a novel, presumably singlet local bound state, resulting from the hybridization of the atomic f-electron wavefunctions with p and/or d orbitals from the

neighbours. Whereas the intermultiplet transitions exhibit considerable broadening due to the finite lifetime of each valence state, the peak at 14 meV is resolution limited, suggesting that it is associated with a true quantum-mechanical eigenstate of MV SmB_6. From a comparison of the spectra collected at different Q-vectors parallel to the main symmetry directions of the crystal, this state is shown to be strongly anisotropic. The excitation exhibits some weak dispersion and modulation in intensity, suggesting that the excitonic 'clouds' formed around each Sm ion slightly interact with each other. A strong temperature dependence of both the intensity and the linewidth is also observed. Since f–d (f–p) hybridization is presumably the leading mechanism for forming the MV eigenstate, delicate changes in the electronic band structure as a function of temperature may be responsible for this effect. Alternatively, the thermal excitation of even a small number of electrons into the conduction band may destabilize the local bound state as the low-carrier character of the system is gradually lost.

Acknowledgments

This work is dedicated to Jean Rossat-Mignod, in memory of his deep scientific insight and outstanding human qualities. We are grateful to A S Mishchenko, K A Kikoin, T Kasuya and A Yu Rumyantsev for stimulating discussions, and to N Pyka, G Engel, E S Clementyev and E V Nefeodova for their help in experiments and data treatment. PAA wishes to thank the LLB for its hospitality. This work was supported by the Russian Foundation for Fundamental Research (project 93-02-2582).

References

[1] Vainshtein E E, Blokhin S M and Paderno Yu B 1965 *Sov. Phys.–Solid State* **6** 2318
[2] Guntherodt G, Thompson W A, Holtzberg F and Fisk Z 1982 *Valence Instabilities* ed P Wachter and H Boppart (Amsterdam: North-Holland) p 313
[3] Allen J W, Batogg B and Wachter P 1979 *Phys. Rev.* B **20** 4807
[4] Kunii S 1987 *J. Magn. Magn. Mater.* **63–64** 673
[5] Cohen R L, Eibschutz M and West K W 1970 *Phys. Rev. Lett.* **24** 386
[6] Tarascon J M, Isikawa Y, Chevalier B, Etourneau J, Hagenmuller P and Kasaya M 1980 *J. Physique* **41** 1141
[7] Mott N F 1973 *Phil. Mag.* **30** 403
[8] Martin R M and Allen J M 1979 *J. Appl. Phys.* **50** 7561
[9] Kasuya T 1976 *J. Physique Coll.* **37** C4 26
Kasuya T, Takegahara K and Fujita T 1979 *J. Physique Coll.* **40** C5 308
[10] Kasuya T 1994 *Europhys. Lett.* **26** 277, 283
[11] Kikoin K A and Mishchenko A S 1990 *J. Phys.: Condens. Matter* **2** 6491
[12] Alekseev P A, Ivanov A S, Dorner B, Shober H, Kikoin K A, Mishchenko A S, Lazukov V N, Konovalova E S, Paderno Yu B, Rumyantsev A Yu and Sadikov I P 1989 *Europhys. Lett.* **10** 457
[13] Holland-Moritz E and Kasaya M 1986 *Physica* B **136** 424
[14] Alekseev P A, Ivanov A S, Lazukov V N, Sadikov I P and Severing A 1992 *Physica* B **180–181** 281
[15] Alekseev P A, Lazukov V N, Osborn R, Rainford B D, Sadikov I P, Konovalova E S and Paderno Yu B 1993 *Europhys. Lett.* **23** 347
[16] Alekseev P A, Mignot J-M, Rossat-Mignod J, Lazukov V N and Sadikov I P 1993 *Physica* B **186–188** 334
[17] Mignot J-M, Alekseev P A, Rossat-Mignod J, Lazukov V N and Sadikov I P 1994 *Physica* B **199–200** 430
[18] Evidence for true excitations of electron–phonon origin was actually discovered at much larger momentum transfers ($Q \approx 6$ Å^{-1}) [12, 14], owing to the Q^2 amplification factor
[19] Al'tschuler T S, Khaliullin G G and Khomskii D I 1986 *Sov. Phys.–JETP* **63** 1234 (Engl. transl. 1986 *Zh. Eksp. Teor. Fiz.* **90** 2104)

[20] Takigawa M, Yasuoka H, Tanaka T, Ishizawa Y, Kasaya M and Kasuya T 1983 *J. Magn. Magn. Mater.* **31–34** 391
[21] Holland-Moritz E, Zirngieble E and Blumenroder S 1988 *Z. Phys.* B **70** 395
[22] Weber W, Holland-Moritz E and Fisher K 1989 *Europhys. Lett.* **8** 257
[23] Moon R M, Koehler W C, McWhan D B and Holtzberg F 1982 *J. Appl. Phys.* **49** 2107
[24] Boucherle J-X, Alekseev P A, Gillon B, Mignot J-M, Lazukov V N, Sadikov I P, Konovalova E S and Paderno Yu B 1994 *Physica* B at press
[25] Shapiro S M and Grier B H 1982 *Phys. Rev.* B **25** 1457
[26] Kasuya T 1994 *J. Phys. Soc. Japan* **63** 2037
[27] Mason T E, Aeppli G, Ramirez A R, Clausen K N, Broholm C, Stücheli N, Bucher E and Palstra T T M 1992 *Phys. Rev. Lett.* **69** 490
[28] Kadowaki H, Sato T, Yoshizawa H, Ekino T, Takabatake T, Fujii H, Regnault L P and Isikawa Y 1994 *J. Phys. Soc. Japan* **63** 2074
[29] Czycholl G 1982 *Phys. Rev.* B **25** 3413
[30] Fedro A J and Sinha S K 1981 *Valence Fluctuations in Solids* ed L M Falikov, W Hanke and M B Maple (Amsterdam: North-Holland) p 329
[31] Osborn R, Lovesey S W, Taylor A D and Balkar E 1991 *Handbook of Physics and Chemistry of Rare Earths* vol 19, ed K A Gschneidner and L Eyring (Amsterdam: Elsevier) p 1